JOURNAL OF APPLIED ELECTROCHEMISTRY 16 (1986) 213–222

Electrochemical synthesis using reactant-incorporated graphite powder electrodes: the reduction of p-dinitrobenzene in dilute aqueous acid

R. H. DAHM, R. J. LATHAM, S. E. MOSLEY

School of Chemistry, Leicester Polytechnic, PO Box 143, Leicester, LE1 9BH, UK

Received 15 January 1985; revised 15 April 1985

An approach to electro-organic synthesis has been developed using a composite or multiphase electrode where the solid, insoluble reactant is incorporated into a compacted powder electrode system. This has been achieved by intimately mixing the finely dispersed organic solid into a paste with graphite powder and an aqueous electrolyte. The paste was then spread between a graphite felt sandwich. A cell capable of utilizing 500 mg of organic material and achieving current densities of 3 A dm^{-2} (6 A g^{-1} of organic material) has been developed, and in such a system *p*-dinitrobenzene has been reduced to *p*-nitrophenylhydroxylamine in 1 M H_2SO_4 (28% yield). Reduction at a potential 100 mV more cathodic than that required for the production of *p*-nitrophenylhydroxylamine, followed by reoxidation at +580 mV, gave *p*-benzoquinone with 34% yield. The electrode performance has been found to depend on its overall thickness, the size of the particles and the graphite content.

1. Introduction

The construction of electrodes by incorporating an electroactive species in a carbon paste allows reactions to take place *in situ*, providing ease of product extraction and reducing mass transport problems. These advantages make the concept attractive for application in electro-organic synthesis but to date this type of application seems to have been largely ignored.

Composite electrodes have, however, been put to use in a number of other applications. They were first reported by Kuwana in 1964 [1, 2], and consequently employed in the electrochemical quantitative and qualitative analysis of iron oxides [3] and silver halides [4, 5]. The electroactive solids were dispersed in a viscous inert liquid such as Nujol and then mixed with graphite powder to form a paste. The active species were then thought to be reacting in the dissolution state. The technique was further developed, for systems in which the reacting solid was totally insoluble in the electrolyte, by using the electrolyte as the electrode binder. Whether or not the electroactive species were then reacting in the solution phase or in the solid-state via a three-component interface (solid reactant/graphite/electrolyte) has not always been easy to establish [6, 7]. Nevertheless, this latter technique has been successfully applied to the quantitative determination of uranium in ores [8], and to the electrochemical analysis of the highly insoluble manganese oxides [9] and sulphide ores [10, 11]. Likewise, Lamache and co-workers [12, 13] have studied and characterized the non-stoichiometric, highly conducting, halide salts of tetrathiafulvalene. Similar electrodes containing easily reducible quinones have also been used as cathodes in experimental secondary cells [14, 15], and under these conditions 100% of the quinone incorporated in an electrode could be reversibly reduced. More recently, work has been carried out on the feasibility of using these electrodes as cathodes in lithium batteries [16].

In this work the synthetic utility of the technique was evaluated by investigating the reduction of *p*-dinitrobenzene (*p*-DNB) in 1 mol dm^{-3} H_2SO_4 on the 10 mg–0.5 g scale.

0021–891X/86 $03.00 + .12

This solid was chosen because of its low solubility in water ($0.12\,g\,l^{-1}$) [17], its low reduction potential [18] and the possibility of the acquisition of more than one product by altering the conditions. Numerous studies of the electrochemical reduction of *p*-DNB in acid have been previously carried out, mainly in ethanolic solution [19–23], and some nitroaromatic compounds have been incorporated into composite electrodes [24, 25] with limited success.

2. Experimental details

2.1. *Electrochemical measurements*

Cyclic voltammetry was carried out using a Wenking ST72 potentiostat coupled to a Wenking VSG 72 voltage scan generator, and results recorded on a J. J. Lloyd PL4 x–y chart recorder. The same potentiostat was also employed in constant potential electrolysis and integration of peaks was by triangulation. All potentials were measured against a saturated calomel electrode (SCE).

2.2. *Preparation of active material*

To make the active electrode material the organic solids (BDH Ltd) were mixed intimately and finely ground with graphite powder (synthetic graphite BDH Ltd). On a small scale (up to ~ 100 mg of total active mass) a vibrating ball mill (Vibromill) was found to provide the quickest and easiest method of doing this. For most solids 30 min vibromilling was sufficient. On a larger scale the operation was carried out either in a micronizing mill (McCrone Research Ltd), usually for 2 h, or in a simple ball mill consisting of a steel capsule and ball bearings shaken in a mechanical flask shaker, usually for 5 h. Up to 10 g of active mass could be made in these devices.

2.3. *Cells*

The two cells used are shown in Figs. 1 and 2. The graphite felt (RVG 1000 Le Carbone) was prewetted in a very dilute solution of electrolyte and Triton X-100 (Octylphenyl

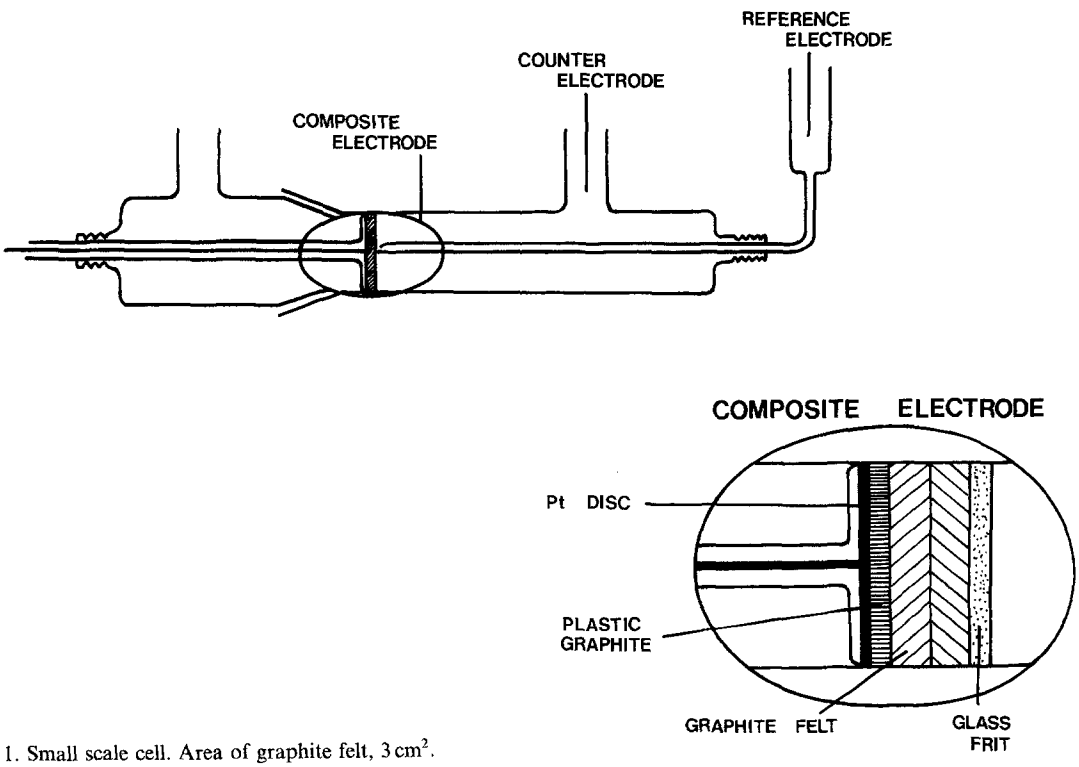

Fig. 1. Small scale cell. Area of graphite felt, $3\,cm^2$.

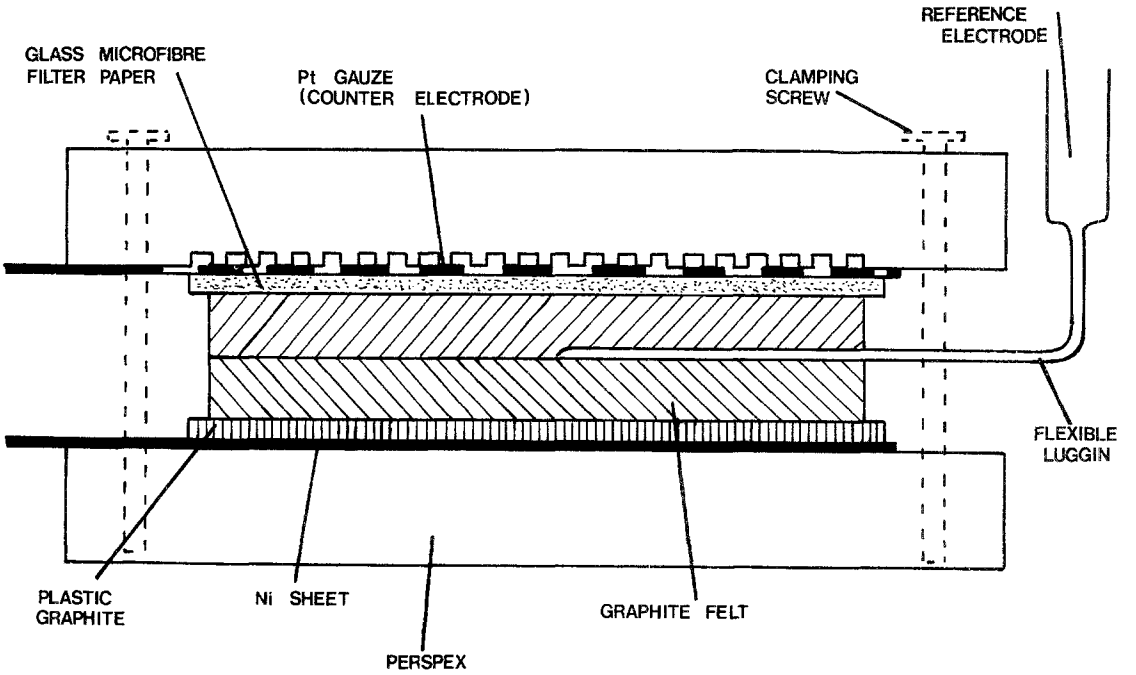

Fig. 2. Preparative cell. Area of graphite felt, $10 \times 10\,cm^2$.

$(Etheneoxide)_{10}$), and the active mass was sprinkled evenly on the felt. The glass microfibre filter paper (Whatman GF/C), was presoaked in electrolyte and was chosen because of its high retention and rapid flow properties. In the preparative cell a gauze counter electrode was employed so that bubbles of evolved gas could escape into channels cut in the cell top, and to maintain electrical conduction a cotton thread was placed in the Luggin capillary.

3. Results and discussion

3.1. *Electrode performance and optimum composition*

Cyclic voltammetric studies with electrodes containing chloranil were carried out in order to obtain the optimum electrode composition (i.e. 100% reactant utilization). The low reduction potential of this quinone (422 mV) [15] allowed integration of cyclic voltammetric peaks without complications due to electrolysis of the electrolyte. For synthetic purposes it was found that an active mixture of up to 33% (mass) chloranil gave optimum utilization. There was no advantage in vibromilling the active mixture for longer than 30 min (Fig. 3), corresponding to a particle size of $< 5\ \mu m$ (measured by optical microscopy), and there also seemed to be no worthwhile advantage in using a concentration of organic material greater than $5\,mg\,cm^{-2}$ of geometrical area of felt (15 mg total active mass cm^{-2}) (Fig. 4). For investigative and analytical purposes a loading of 2% (mass) was used, usually in a total active mass of 10 mg. This gave a chloranil density of $6.7 \times 10^{-2}\,mg\,cm^{-2}$ of graphite felt.

The electrode composition determined the shape of cyclic voltammetric peaks. This is demonstrated in the variation of the peak potentials (E_p) of the two reduction steps of *p*-DNB (Tables 1–3). The values of E_p ultimately become independent at low *p*-DNB loadings, although still dependant on potential scan rate. It therefore appears that the IR drop within the working electrode exerts a pronounced effect on the observed peak potentials. However, these effects are minimized by the use of low reactant loadings and initial cyclic voltammograms were therefore obtained using, in all cases, mass loadings of only 2%.

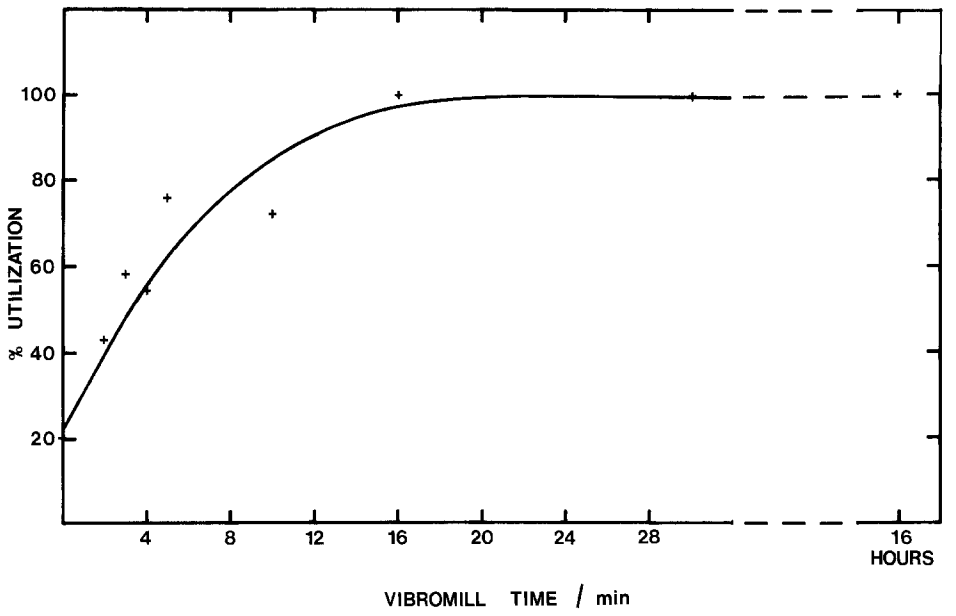

Fig. 3. Variation of percentage chloranil utilization with vibromilling time. Percentage utilization from integration of cyclic voltammetric peaks in 1 M H_2SO_4. Chloranil, 17 mg; graphite powder, 33 mg; scan rate, 0.3 mV s^{-1}; electrode area, 3 cm^2.

3.2. *Attainable potential ranges*

In determination of the useful potential ranges of the electrodes in aqueous electrolytes, cyclic voltammetry on pure graphite electrodes was employed in a series of buffer solutions of high buffer capacity. Potential sweeps starting from the equilibrium potential were taken into hydrogen and oxygen evolution potentials. The limits (Table 4) were then arbitrarily taken as

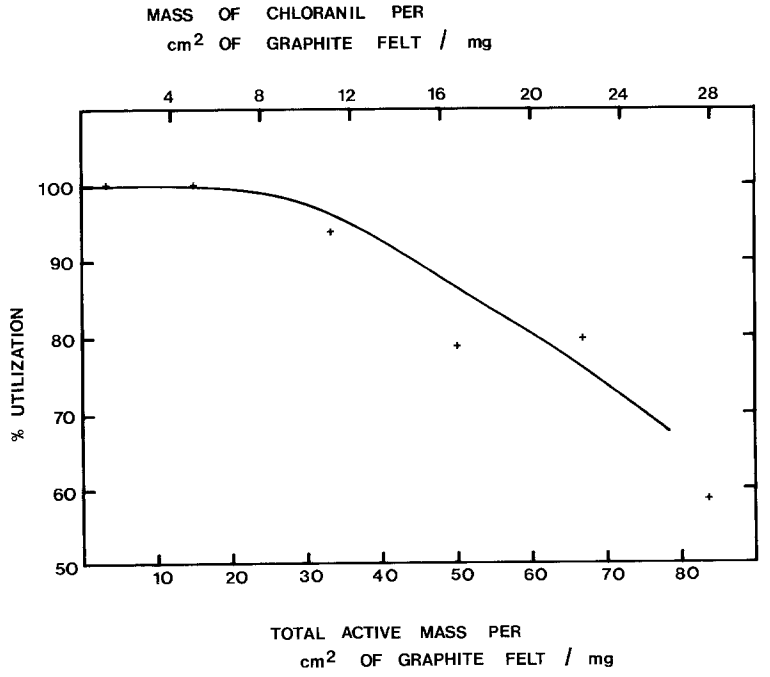

Fig. 4. Variation of percentage chloranil utilization with reactant concentration per geometrical area of felt. Percentage utilization from integration of cyclic voltammetric peaks in 1 M H_2SO_4. Chloranil electrodes, 33% (mass); area, 3 cm^2; scan rate, 0.3 mV s^{-1}.

Table 1. Variation of reduction peak potentials of p-*DNB with voltage scan rate*

Active mass (mg)			*CV scan rate* ($mV\,s^{-1}$)	*First reduction potential (mV(SCE))*	*Second reduction potential (mV(SCE))*
p-*DNB*	*Graphite*	*Total*			
5	10	15	1.0	−185	−370
5	10	15	0.1	−105	−230
5	10	15	0.01	−60	−180

Table 2. Variation of reduction peak potentials of p-*DNB with graphite content*

Active mass (mg)			*CV scan rate* ($mV\,s^{-1}$)	*First reduction potential (mV(SCE))*	*Second reduction potential (mV(SCE))*
p-*DNB*	*Graphite*	*Total*			
16	34	50	0.1	−100	−230
8	42	50	0.1	−85	−215
1	49	50	0.1	−25	−110
0.25	50.0	50.25	1.0	−40	−290
0.2	10.0	10.2	1.0	−20	−185

being the potential when the current density was 20% of the peak current density obtained with a 3 cm^2 graphite felt electrode containing 16 mg chloranil (34 mg graphite) in 1 M H_2SO_4 cycled at the same sweep rate (1 $mV\,s^{-1}$). One important result was that obtained at pH < 2 (Fig. 5). The graphite surface is then oxidized irreversibly at +950 mV (SCE), as previously reported [26]. Electrodes held potentiostatically at +1.0 V for 1 h seemed to have undergone irreversible oxidation in that time since the current density had dropped to virtually zero. This should be taken into account if a species with an oxidation potential of > +900 mV is to be studied in acid.

Electrochemical reactions occurring at potentials outside the limits cannot be studied in aqueous electrolytes but non-aqueous electrolytes can be used [16].

3.3. *Reduction of* p-*dinitrobenzene*

Cyclic voltammetry between +750 mV and −250 mV (SCE) was carried out on *p*-dinitrobenzene (*p*-DNB) in 1 M H_2SO_4. The voltammogram of an electrode containing 6.7×10^{-2} mg of *p*-DNB per cm^2 of graphite felt (Fig. 6) was very similar to that obtained in the preparative cell with a higher reactant density, 5 $mg\,cm^{-2}$ (Fig. 7). Due to the greater organic loading in the latter case, the peaks were broader and the reduction peak potentials had shifted to more negative values, even at the slower sweep

Table 3. Variation of reduction peak potentials of p-*DNB with amount of* p-*DNB incorporated into the electrode*

Active mass (mg)			*CV scan rate* ($mV\,s^{-1}$)	*First reduction potential (mV(SCE))*	*Second reduction potential (mV(SCE))*
p-*DNB*	*Graphite*	*Total*			
5	10.0	15.0	1	−185	−370
0.2	10.0	10.2	1	−20	−185
0.05	10.0	10.05	1	−20	−190

Table 4. Attainable potential ranges

Electrolyte	*Anodic limit mV(SC)*	*Cathodic limit mV(SCE)*
1 M H_2SO_4	+1800	−325
*pH 2.4 buffer**		
0.2 M H_3PO_4	+1450	−450
0.2 M NaH_2PO_4		
0.2 M Na_2SO_4		
*pH 4.8 buffer**		
0.2 M CH_3CO_2H	+1350	−700
0.2 M CH_3CO_2Na		
0.2 M Na_2SO_4		
pH 6.8 buffer		
0.2 M NaH_2PO_4	+1300	−800
0.2 M Na_2HPO_4		
pH 9.6 buffer		
0.2 M $NaHCO_3$	+1050	−1000
0.2 M Na_2CO_3		
pH 12.3 buffer		
0.2 M Na_2HPO_4	+875	−1025
0.2 M NaOH		
2 M NaOH	+500	−1100

* Na_2SO_4 added to keep buffer solutions at constant ionic strength.
From cyclic voltammograms of pure graphite powder (30 mg) electrodes, 3 cm^2. Scan rate, 1 mV s^{-1}.

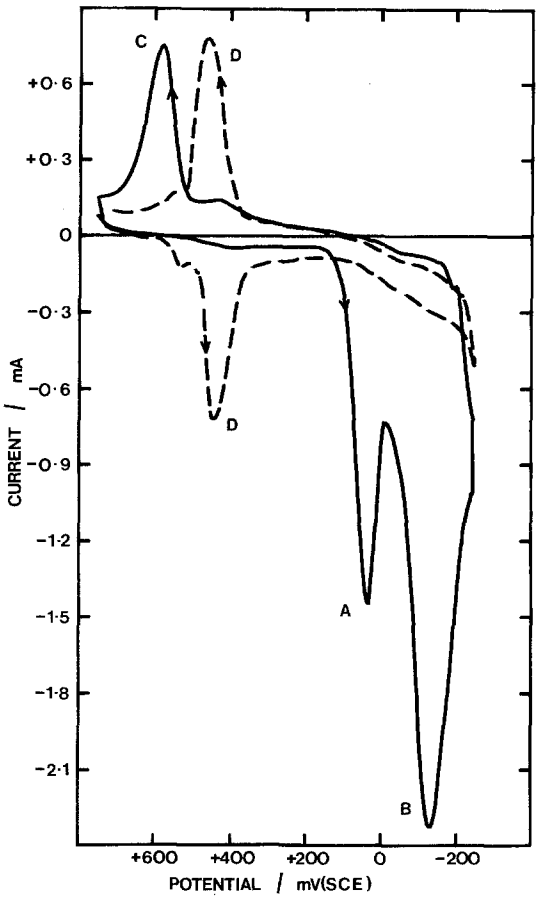

Fig. 6. Cyclic voltammogram of *p*-DNB electrode (3 cm^2) in 1 M H_2SO_4. *p*-DNB, 0.2 mg; graphite powder, 10 mg; scan rate, 1 mV s^{-1}. ——, first cycle; – – –, second cycle.

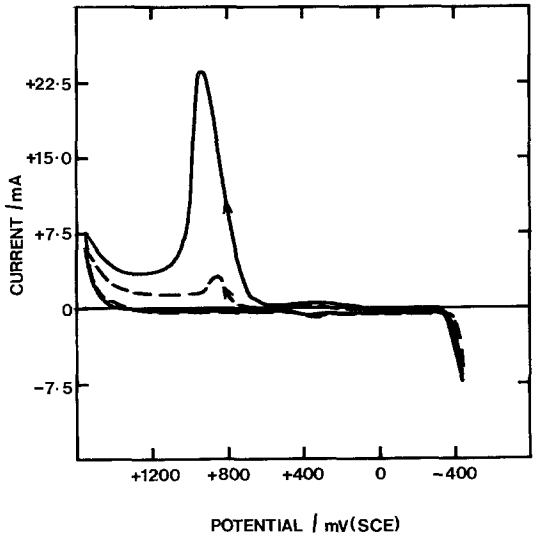

Fig. 5. Cyclic voltammogram of graphite powder (30 mg) in 1 M H_2SO_4. Electrode area, 3 cm^2. Scan rate, 0.3 mV s^{-1}. ——, first cycle; – – –, second cycle.

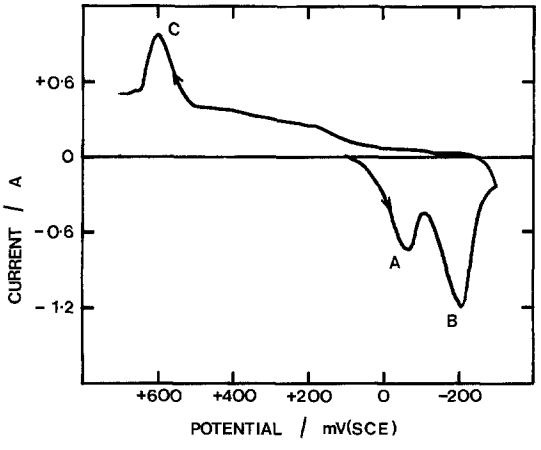

Fig. 7. Cyclic voltammogram of *p*-DNB electrode (100 cm^2 in preparative cell) in 1 M H_2SO_4. *p*-DNB, 500 mg; graphite powder, 1 g; scan rate, 0.1 mV s^{-1}.

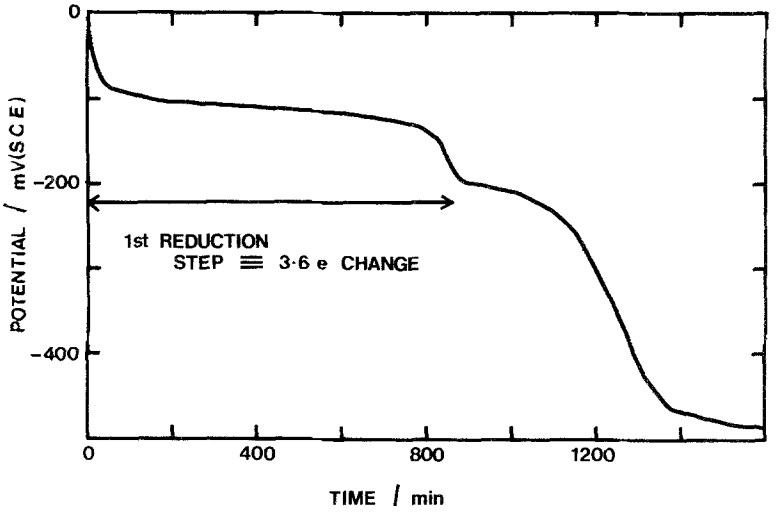

Fig. 8. Potential–time curve of *p*-DNB electrode (3 cm^2) in 1 M H_2SO_4. *p*-DNB, 5 mg; graphite powder, 10 mg; charge rate, 0.25 mA (50 mAg^{-1} of *p*-DNB).

rate. Integration of the first reduction peak indicated a four-electron change for this step, and this was confirmed by galvanostatic measurements (Fig. 8). This corresponds to the reduction of one of the nitro groups to give *p*-nitrophenylhydroxylamine (*p*-NPH), similar to the electrochemical reduction of mononitrobenzene in aqueous acid/ethanol solution [27]. The reaction is thought to proceed either via a quinoidal intermediate I [19] or a hydrated nitroso derivative II [20].

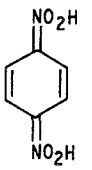

I

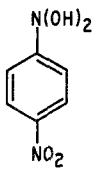

II

Cyclic voltammetry on *p*-NPH, prepared according to Kuhn and Weygand [28], indicated that it indeed was the first reduction product of *p*-DNB. When reduced it gave peaks corresponding to B, C, D and D′ obtained with *p*-DNB (cf. Figs 6, 9), and when oxidized gave couples E/E′ and F/F′ (Fig. 10) which were likewise obtained (Fig. 11) when a cyclic sweep of *p*-DNB was reversed after peak A. It is suggested

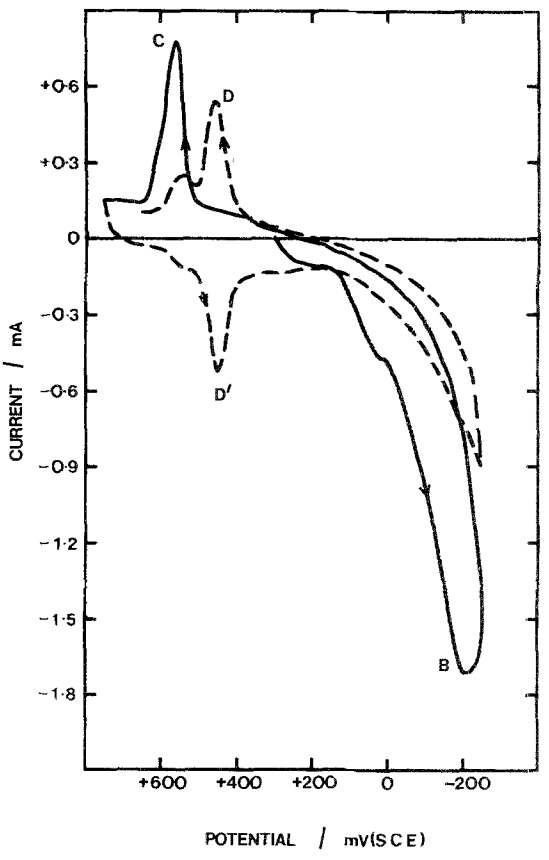

Fig. 9. Cyclic voltammogram of *p*-NPH electrode (3 cm^2) in 1 M H_2SO_4. *p*-NPH, 0.2 mg; graphite powder, 10 mg; scan rate, 1 mVs^{-1}. ——, first cycle; – – –, second cycle.

that E/E′ is likely to be due to

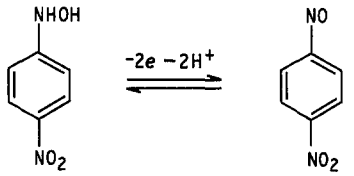

This occurs in methanolic solution (pH 1) at an equilibrium potential of +375 mV [23]. The original of the couple F/F′ is not known but may be due to products formed by coupling of the above intermediates.

The preparative cell was used to prepare *p*-NPH by electrolysing *p*-DNB at a constant potential of −50 mV (approximate half-wave potential of first reduction peak measured in preparative cell, Fig. 7) using 1 mol dm^{-3} H_2SO_4 electrolyte. Utilization of 500 mg of *p*-DNB (incorporated in 1 g of graphite) took 45 min, with a maximum current density of 3 A dm^{-2} (6 Ag^{-1} of *p*-DNB). The product was extracted into ether after neutralization with saturated bicarbonate solution to yield crude *p*-NPH (melting point 101–104° C), 86% chemical yield. Two recrystallizations from benzene under nitrogen gave a pure product, melting point 107° C [28, 29], yield 28%. Characterization was by mass spectrometry: m/e 154 (100%), 124 (34%),

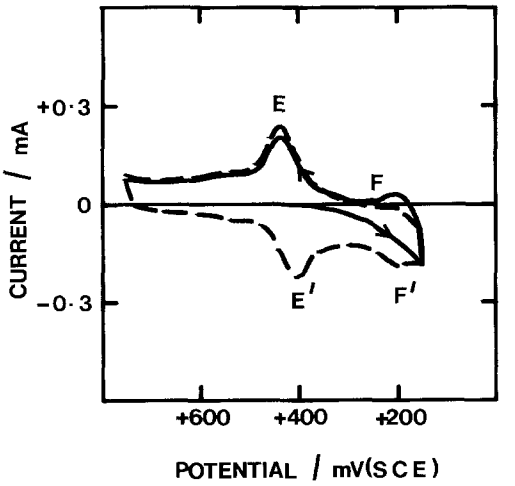

Fig. 10. Cyclic voltammogram of *p*-NPH electrode (3 cm^2) in 1 M H_2SO_4. *p*-NPH, 0.2 mg; graphite powder, 10 mg; cathodic limit +150 mV; scan rate, 1 mV s^{-1}. ——, first cycle; – – –, second cycle.

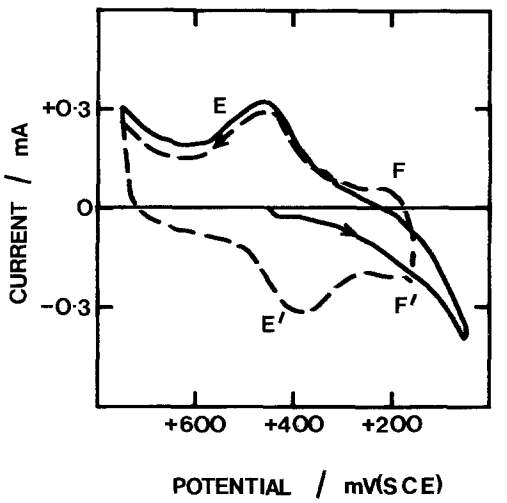

Fig. 11. Cyclic voltammogram of *p*-DNB electrode (3 cm^2) in 1 M H_2SO_4. *p*-DNB, 0.2 mg; graphite powder, 10 mg; cathodic limits +50 mV (first cycle, ——), +150 mV (second cycle, – – –); scan rate, 1 mV s^{-1}.

91 (61%), 63 (39%), 64 (36%), 30 (48%), 28 (41%); and infra-red analysis (KBr Disc), major bands 3315, 3300, 3240, 1605, 1510, 1340, 1120 and 1030 cm^{-1}.

Tallec [21, 22] assigned the product obtained by electrolysing *p*-DNB at a mercury cathode in H_2SO_4 (aq)/ethanol solutions as being *p*-NPH. Its melting point was given as 122° C which differs from the value of 107° C reported by both Kuhn and Weygand [28] and Entwhistle *et al.* [29], and which is also the value of the melting point of the compound isolated in this work.

The second reduction step of *p*-DNB (peak B, Figs 6, 7) was due to an eight-electron reduction of *p*-NPH (by integration of voltammetric peaks) which presumably gave *p*-phenylenediamine (*p*-PDA). The actual mechanism of *p*-PDA formation has been subject to debate. A polarographic study of the reduction of *p*-DNB was made by Heyrovsky *et al.* [19] who proposed that *pp′*-dinitroazoxybenzene was an intermediate, and Darchen [30] has suggested other alternatives, but no intermediates were isolated in either case.

Cyclic voltammetry showed that the reduction product corresponding to peak B (Fig. 6) could be oxidized (peak C) to form a product that underwent a chemical reaction to give a new redox couple, D/D′, centring on

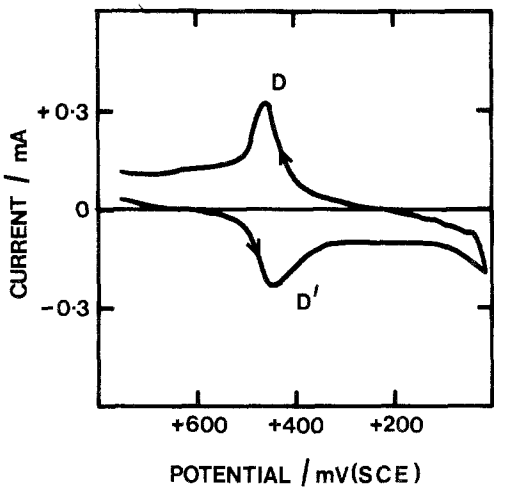

Fig. 12. Cyclic voltammogram of *p*-BQ electrode (3 cm^2) in 1 M H_2SO_4. *p*-BQ, 0.2 mg; graphite powder, 10 mg; scan rate, 1 mV s^{-1}.

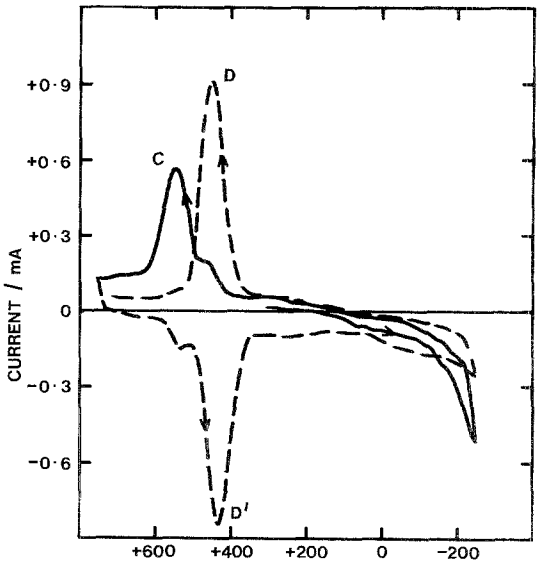

Fig. 13. Cyclic voltammogram of *p*-PDA electrode (3 cm^2) in 1 M H_2SO_4. *p*-PDA, 0.2 mg; graphite powder, 10 mg; scan rate, 1 mV s^{-1}. ——, first cycle; – – –, second cycle.

+420 mV. This was identical to the *p*-benzoquinone/hydroquinone redox couple (cf. couple D/D′ Figs 6, 12). *p*-Benzoquinone (*p*-BQ) is known to be formed by the acid-catalysed hydrolysis of *p*-benzoquinone-diimine [31], the oxidation product of *p*-PDA in acid [23]. *p*-BQ itself was synthesized in the preparative cell by reducing *p*-DNB at a constant potential of −150 mV for 30 min and subsequently oxidizing the *p*-PDA produced at +600 mV for 10 min. The product was extracted as described above and purified by vacuum sublimation. Characterization was by IR analysis and 500 mg of *p*-DNB yielded 109 mg (34%) of *p*-BQ, melting point 113–115° C. The yield was very good considering the number of steps in the reaction. The existence of *p*-PDA as an intermediate in the *p*-BQ preparation was indicated by cyclic voltammetry of commerical *p*-PDA (Fig. 13) which gave peaks C, D and D′.

The cyclic voltammetric pattern of *p*-DNB found in this work is similar to that reported by Jannakoudakis and Theodoridou [23] using aqueous/methanol and carbon fibre electrodes, but no *p*-BQ was reported to be formed although the *p*-PDA/*p*-benzoquinonediimine couple was observed. This was due to the very much greater potential scan rates used in [23].

One interesting feature is the fact that *p*-NPH is soluble in 1 M H_2SO_4. Electrodes containing this compound posed no problems if used soon after assembly (i.e. up to 2 h), otherwise the reactant was found to leach out of the electrode. Fig. 10 illustrates this point (i.e. the small amount of *p*-NPH further reduced). It therefore seems likely that the electrochemical reactions of this compound were occurring mainly in the solution state.

3.4. *Applicability of cyclic voltammetry to reactant incorporated graphite powder electrodes*

Although no comprehensive theoretical treatment of cyclic voltammetry applied to composite electrodes has appeared, this technique is nevertheless useful as an initial investigative tool. The number of individual charge transfer steps is clearly shown and in favourable cases peak integration yields information on the number of electrons transferred. The electrochemical process can frequently be reversed, often with nearly 100% utilization. In such cases the observed equilibrium potential is independant of sweep rate and composition over a wide range and is in close agreement with values obtained using conventional methods [32]. The technique is also useful for the study of follow up reactions as shown in Fig. 4.

4. Conclusion

Graphite powder electrodes which incorporate solid, insoluble reactants and which are porous to the electrolyte provide a convenient method for the study of electrochemical reactions of insoluble compounds and can be used for electro-organic synthetic purposes. This has been shown by the study of the reduction of *p*-dinitrobenzene in aqueous acid, and the synthetic production of *p*-nitrophenylhydroxylamine, and also of *p*-benzoquinone which could be obtained by *in situ* reoxidation of further reduction products. Advantages of this approach to electrochemical synthesis include large product yields and high current densities. The electrode performance depends on:

1. The ratio of organic material to graphite
2. Particle size
3. The active mass per unit geometrical area of graphite felt

When the solid reactant is insoluble in the electrolyte then the electrochemical reactions may occur mainly in the solid state and these processes may be limited to simple redox reactions involving electrons and proton transfer only. EC reactions involving intermolecular coupling are currently under investigation.

Acknowledgement

Leicestershire County Council are thanked for a research assistantship to SEM.

References

[1] T. Kuwana and W. G. French, *Anal. Chem.* **36** (1964) 241.
[2] F. A. Shultz and T. Kuwana, *J. Electroanal. Chem.* **10** (1965) 95.
[3] J. M. Lecuire, *ibid.* **66** (1975) 195.
[4] W. R. Ruby and C. G. Tremmel, *ibid.* **18** (1968) 231.
[5] S. Meseric and E. A. M. F. Dahman, *Anal. Chim. Acta* **64** (1973) 431.
[6] E. Laviron, *J. Electroanal. Chem.* **90** (1978) 33.
[7] D. Bauer and P. Gaillochet, *Electrochim. Acta* **19** (1974) 597.
[8] P. Gaillochet, D. Bauer and M. C. Henrion, *Analysis* **3** (1975) 513.
[9] F. Chouaib, O. Cauquil and M. Lamache, *Electrochim. Acta* **26** (1981) 325.
[10] M. Lamache, D. Kende and D. Bauer, *Nouv. J. Chim.* **1** (1977) 377.
[11] M. C. Brage, M. Lamache and D. Bauer, *Electrochim. Acta* **24** (1979) 25.
[12] M. Lamache, H. Menet and A. Moradpour, *J. Amer. Chem. Soc.* **104** (1982) 4520.
[13] M. Lamache, R. Najean, *Electrochim. Acta* **29** (1984) 273.
[14] H. Alt, H. Binder, G. Klempert, A. Köhling and G. Sandstede, *J. Appl. Electrochem.* **2** (1972) 193.
[15] H. Binder, R. Knodler, A. Köhling, G. Sandstede and G. Walter, *Power Sources* **6** (1976) 643.
[16] S. Tobishima, J. Yamaki and A. Yamaji, *J. Appl. Electrochem.* **14** (1984) 721.
[17] Beilstein's 'Handbuch der Organischen Chemie', 4th edn, Vol. 5 EIII. Springer, Berlin (1964).
[18] J. Pearson, *Trans. Faraday Soc.* **44** (1948) 683.
[19] M. Heyrovsky, S. Vauricka and L. Holleck, *Coll. Czech. Chem. Comm.* **36** (1971) 971.
[20] A. Darchen and C. Moinet, *J. Electroanal. Chem.* **78** (1977) 81.
[21] A. Tallec, *Ann. Chim.* **3** (1969) 155.
[22] *Idem, ibid.* **4** (1968) 67.
[23] P. D. Jannakoudakis and E. Theodoridou, *Z. Phys. Chem.* **130** (1982) 49.
[24] M. A. Gutjahr and K. D. Beccu, *Chem.-Ing.-Tech.* **4** (1970) 202.
[25] M. V. King, *J. Org. Chem.* **26** (1961) 3323.
[26] R. E. Panzer and P. J. Elving, *Electrochim. Acta* **20** (1975) 635.
[27] A. Darchen and C. Moinet, *J. Electroanal. Chem.* **68** (1976) 173.
[28] R. Kuhn and F. Weygand, *Ber.* **69** (1936) 1969.
[29] I. D. Entwhistle, T. Gilkerson, R. A. W. Johnstone and R. P. Telford, *Tetrahedron* **34** (1978) 213.
[30] A. Darchen, *Compt. rend. Acad. Sci. Ser. C* **272** (1971) 2193.
[31] L. K. J. Tong, *J. Phys. Chem.* **58** (1954) 1090.
[32] W. M. Clark, 'Oxidation–Reduction Potentials of Organic Systems', Williams and Wilkins, Baltimore (1960).